

Exactly solvable model of Ising-Heisenberg diamond-chain with $S = 1$ XXZ vertical dimers with additional biquadratic interactions and single-ion anisotropy

Onofre Rojas¹ S. M. de Souza¹, Vadim Ohanyan^{2,3} and Martiros Khurshudyan²

¹*Departamento de Ciencias Exatas, Universidade Federal de Lavras, CP 3037, 37200000, Lavras, MG, Brazil*

²*Yerevan State University, A. Manoogian, 1, Yerevan, 0025 Armenia*

³*Yerevan Physics Institute, Alikhanian Br.2, Yerevan, 0036, Armenia*

E-mails: ors@dex.uflla.br, ohanyan@yerphi.am

Abstract

An exactly solvable variant of diamond chain with mixed $S = 1$ and $S = 1/2$ spins is considered. Vertical $S = 1$ dimers are taken as quantum ones with Heisenberg bilinear and biquadratic interactions and with single-ion anisotropy, while all interactions between $S = 1$ spins and $S = 1/2$ spins residing on the intermediate sites are taken in the Ising form. Solving the model exactly within classical transfer-matrix formalism we obtain an exact expressions for all thermodynamic function of the system. The detailed analysis of the $T = 0$ ground state phase diagram is presented as well as the exact plots of various thermodynamic functions, emphasizing the effect of biquadratic term.

1 Introduction

Lattice models of quantum magnetism continue to be in the focus of attention of theoretical condensed matter physicists. Beside of great practical importance connected with description of magnetic and thermodynamic properties of real magnetic materials, this research area is also attractive from the general statistical mechanics and strongly correlated system theory points of view, especially when one deals with exactly solvable strongly interacting many-body system. The diamond chain is a one-dimensional lattice spin system in which the vertical spin dimers alternate with single spins (See figure 1). This model with $S = 1/2$ is believed to describe the magnetic lattice of mineral azurite, $\text{Cu}_3(\text{CO}_3)_2(\text{OH})_2$, which is famous for its deep blue pigmentation [1, 2, 3, 4]. Theoretical research of various aspects of diamond chain physics received much attention during last years [5]-[16]. Diamond chain and especially diamond chain with mixed ($S, S/2$) spin are shown to have very rich ground state phase diagrams with Haldane and several spin-cluster states which are tensor product of exact local eigenstates of cluster spins [5, 6]. Many other issues of diamond chain physics have been investigated theoretically during last years including Dzyaloshinsky-Moriya term influence on magnetization processes [7], multiple-spin-exchange effects [8], magnetization plateaus [9, 10], magnetocaloric effect [11], e.t.c. Very recently another one interesting feature of diamond chain, possibility of localized magnon excitations, has been also investigated [12].

Especially important issue is the effect of frustration, which is rather strong in antiferromagnetic diamond chain because of triangular arrangement of the sites. Variants of frustrated recurrent lattices with diamond plaquette have been also studied in Refs. [21] and [22]. However, diamond chain is not integrable in general. Thus, the exact analysis of the dynamic and especially thermodynamic properties of diamond chain is a very complicated issue. Nevertheless, one can consider various exactly solvable variants of spin systems possessing diamond chain topology of interaction bonds with simplified structure of interactions [13]-[16]. The diamond chain with only Ising type of interaction have been exactly solved within classical transfer-matrix technique in Ref. [13] revealing reach $T = 0$ ground state phase diagram. Yet another exactly solvable diamond chains have been considered in Refs. ([14]-[17]), where vertical spin dimers have been taken as quantum ones with XXZ interaction while interaction between spins localized on vertical dimer sites and spins from the single sites alternating with them is of Ising type. Mapping the system into a single Ising chain within iteration-decoration transformation [18, 19, 20] the authors gave complete description of the ground state properties, $T = 0$ ground state phase diagram as well as thermodynamic functions for all values of vertical dimer spins magnitude S . In a very recent paper the diamond chain with XX -interaction has been considered in the Jordan-Wigner formalism [17].

Considering the mixed spin chains (or another one-dimensional spin systems with more complicated geometry) with Ising and Heisenberg bonds (or even just Ising counterparts of the known quantum spin models) one can achieve two-fold goal: to construct novel exactly solvable lattice spin model which allow one to obtain analytic expression for all thermodynamic functions of the model, and to get an approximate models which can be useful for understanding the properties of underlying purely quantum models [14, 15, 16, 23, 24, 25, 26, 27, 28, 29]. Exact thermodynamic solutions of such models even can shed a light to the properties of real magnetic materials. For instance, for alternating spin chain

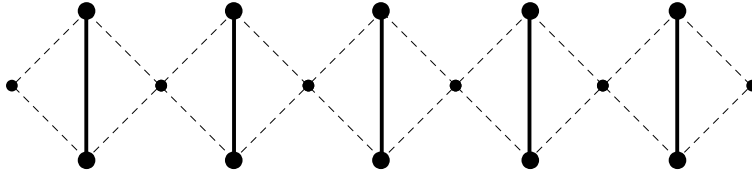


Figure 1: The diamond chain with Ising and Heisenberg bonds. Solid bold lines denote XXZ quantum bond, dotted lines correspond to Ising interactions. Large(small) circles denote \mathbf{S} (σ) spins.

even simplest models with only Ising interaction can reflect the underlying magnetic behavior of the corresponding Heisenberg counterpart at least in qualitative way [30, 31], moreover, some exactly solvable models with Ising and Heisenberg bonds can also provide satisfactory quantitative picture[29]. Very recently, the synthesis of novel class of trimetallic 3d-4d-4f coordination polymers has been reported. Some compounds of these series are single chain magnets with Ising and Heisenberg bonds [32]. This discovery makes investigation of exact solutions of spin chains with Ising and Heisenberg bonds important form practical point of view.

In this paper we consider mixed spin-(1,1/2) diamond chain with Ising and Heisenberg bonds which extends the system considered in Ref. [16] by including biquadratic term for $S = 1$ XXZ-dimers and single-ion anisotropy. Biquadratic terms are usually originated from the spin-lattice coupling in the adiabatic phonons approximation[33] but also can be considered as the effect of quadrupole interaction between the spins. We do not make any assumption about the origin of biquadratic terms considering them as a part of general Hamiltonian. The model allow one to calculate the partition function and, thus, all thermodynamic quantities exactly within classical transfer-matrix formalism[34]. We present the analysis of $T = 0$ ground-state phase diagrams and plot the curves of magnetization processes for finite temperatures, demonstrating magnetization plateaus at $M = 1/5$ and $M = 3/5$ in the units of saturation magnetization.

The paper is organized as follows. In the second Section we formulate the model and present its eigenvalues. In the third section we describe possible ground states of the system and present the ground-states phase diagram. In section 4 we present its exact solution and discuss the magnetization and thermodynamics properties of the model. Finally in sec. 5 a short summary is followed.

2 The model and its exact solution

Let us consider the system of vertical $S = 1$ spin dimers with Heisenberg XXZ bilinear and biquadratic interactions and uniaxial single-ion anisotropy. These dimers are assembled to the chain by alternating with Ising spins σ , so that each spin S in certain dimer interacts to its both left and right Ising spins via Ising type interaction (See figure 1). So, we have the so-called diamond-chain with $S = 1$ Heisenberg dimers and $\sigma = 1/2$ Ising spins between them. The corresponding Hamiltonian is the sum over the block Hamiltonians:

$$\mathcal{H} = \sum_{i=1}^N \left(\mathcal{H}_i - \frac{h_2}{2} (\sigma_i + \sigma_{i+1}) \right), \quad (1)$$

$$\mathcal{H}_i = J(\mathbf{S}_{i1} \cdot \mathbf{S}_{i2})_\Delta + K(\mathbf{S}_{i1} \cdot \mathbf{S}_{i2})_\Delta^2 + D((S_{i1}^z)^2 + (S_{i2}^z)^2) + J_0(\sigma_i + \sigma_{i+1})(S_{i1}^z + S_{i2}^z) - h_1(S_{i1}^z + S_{i2}^z),$$

where N is the number of the unit cells (blocks with two spin-1 and one spin-1/2), while i correspond the particles at i -cell. J being the coupling constant of bilinear XXZ -interaction between Heisenberg spins, which we assume to be of the following form

$$(\mathbf{S}_{i1} \cdot \mathbf{S}_{i2})_\Delta = \Delta(S_{i1}^x S_{i2}^x + S_{i1}^y S_{i2}^y) + S_{i1}^z S_{i2}^z, \quad (2)$$

whereas K denotes the biquadratic XXZ-interaction term, D means the single ion-anisotropy and J_0 being the purely Ising interaction term. h_2 and h_1 are the external magnetic field acting on σ_i and S_i respectively.

In order to solve this model, at first, we need to diagonalize the block Hamiltonian for arbitrary i -th block. Nine eigenvalues of \mathcal{H}_i , $\lambda_n(\sigma_i, \sigma_{i+1})$, $n = 1 \dots 9$ can be found analytically, which write down as

$$\begin{aligned}
\lambda_1 &= -2h_1 + J + K + 2D + 2J_0(\sigma_i + \sigma_{i+1}), \\
\lambda_2 &= +2h_1 + J + K + 2D - 2J_0(\sigma_i + \sigma_{i+1}), \\
\lambda_3 &= -h_1 + \Delta(J + \Delta K) + D + J_0(\sigma_i + \sigma_{i+1}), \\
\lambda_4 &= +h_1 + \Delta(J + \Delta K) + D - J_0(\sigma_i + \sigma_{i+1}), \\
\lambda_5 &= -h_1 - \Delta(J - \Delta K) + D + J_0(\sigma_i + \sigma_{i+1}), \\
\lambda_6 &= +h_1 - \Delta(J - \Delta K) + D - J_0(\sigma_i + \sigma_{i+1}), \\
\lambda_7 &= -J + K + 2D, \\
\lambda_8 &= \frac{-J + (1 + 4\Delta^2)K + 2D}{2} + \frac{1}{2}\sqrt{8\Delta^2(J - K)^2 + (J - K - 2D)^2}, \\
\lambda_9 &= \frac{-J + (1 + 4\Delta^2)K + 2D}{2} - \frac{1}{2}\sqrt{8\Delta^2(J - K)^2 + (J - K - 2D)^2}.
\end{aligned} \tag{3}$$

The eigenvectors of block Hamiltonian \mathcal{H}_i up to the inversion of all spins are

$$\begin{aligned}
|v_2\rangle &= |1, 1\rangle, & \Rightarrow & \lambda_1, \lambda_2 \\
|v_{1,s}\rangle &= \frac{1}{\sqrt{2}}(|1, 0\rangle + |0, 1\rangle), & \Rightarrow & \lambda_3, \lambda_4 \\
|v_{1,a}\rangle &= \frac{1}{\sqrt{2}}(-|1, 0\rangle + |0, 1\rangle), & \Rightarrow & \lambda_5, \lambda_6 \\
|v_{0,a}\rangle &= \frac{1}{\sqrt{2}}(-| - 1, 1\rangle + |1, -1\rangle), & \Rightarrow & \lambda_7 \\
|v_{0,\pm}\rangle &= \frac{1}{\sqrt{2 + c_{\pm}^2}}(| - 1, 1\rangle + c_{\pm}|0, 0\rangle + |1, -1\rangle), & \Rightarrow & \lambda_8, \lambda_9
\end{aligned} \tag{4}$$

where 1, 0 and -1 in first(second) place stand for the $S^z = 1, 0$ and -1 states for first(second) spin in vertical dimer and the following notation is adopted:

$$c_{\pm} = \frac{1}{2\Delta} \left(1 + \frac{2D \pm \sqrt{8\Delta^2(J - K)^2 + (J - K - 2D)^2}}{K - J} \right). \tag{5}$$

The first eigenvectors of the dimer defined as $|v_2\rangle$ corresponds to the parallel ordered spins with magnetization per site $m_s = 1$, the eigenvector $|v_{1,s}\rangle$ and $|v_{1,a}\rangle$ corresponds to symmetric and antisymmetric states vector respectively, whereas $|v_{0,a}\rangle$ is an antisymmetric state vector with magnetization $m_s = 0$, finally $|v_{0,\pm}\rangle$ are the symmetric eigenvectors with magnetization $m_s = 0$.

The remaining eigenvectors of the eigenvalues λ_2 , λ_4 and λ_6 can be obtaining using the spin inversion.

2.1 Special case $K = J$

At the special value $K = J$ the $S_{tot}^z = 0$ sector of the block Hamiltonian undergoes qualitative changes which can be obtained substituting carefully $K = J$ value into the general solution presented above in eq.(4). This should be considered as a consequence of the special symmetry of the Hamiltonian for these values of parameters, more precisely, the fact that operator $(\mathbf{S}_1 \cdot \mathbf{S}_2)_{\Delta} + (\mathbf{S}_1 \cdot \mathbf{S}_2)_{\Delta}^2$ can be represented in terms of permutation operators P_{12} . In this case the eigenstates $|v_{0,a}\rangle$ and $|v_{0,\pm}\rangle$ of the Hamiltonian reduce to the following ones

$$\begin{aligned}
|v_{0,a}\rangle &= \frac{1}{\sqrt{2}}(|1, -1\rangle - | - 1, 1\rangle), & \Rightarrow & \lambda_7 = 2D, \\
|v_{0,+}\rangle &= |0, 0\rangle, & \Rightarrow & \lambda_8 = 2J\Delta^2, \\
|v_{0,-}\rangle &= \frac{1}{\sqrt{2}}(|1, -1\rangle + | - 1, 1\rangle), & \Rightarrow & \lambda_9 = 2(J\Delta^2 + D).
\end{aligned} \tag{6}$$

Note that a straightforward substitution in eq.(5) could yield to an undefined coefficients of the eigenstates.

3 Phase diagram

Let us describe possible $T = 0$ ground states of the chain under consideration and the corresponding energies per block. Generally speaking, there are $9 \times 2 = 18$ possible ground states for each block. However, if one restricts himself with the ground states which are equivalent up to the inversion of all spins one will arrive at the following spin configurations. The fully polarized state ($M = 1$)

$$|SP\rangle = \prod_{i=1}^N |v_2\rangle_i \otimes |\uparrow\rangle_i, \quad \varepsilon_{SP} = J + K + 2D + 2J_0 - \frac{5}{2}H, \quad (7)$$

where $|\uparrow\rangle_i (|\downarrow\rangle_i)$ stands for the up(down) state of the σ -spin in the i -th block. Hereafter, we also put $h_1=h_2=H$. The next sector of ground states contains three different ferrimagnetic spin configurations with the value of magnetization equal to $3/5$ ($M = 3/5$),

$$\begin{aligned} |F1\rangle &= \prod_{i=1}^N |v_2\rangle_i \otimes |\downarrow\rangle_i, \quad \varepsilon_{F1} = J + K + 2D - 2J_0 - \frac{3}{2}H, \\ |F2\rangle &= \prod_{i=1}^N |v_{1,s}\rangle_i \otimes |\uparrow\rangle_i, \quad \varepsilon_{F2} = \Delta(J + \Delta K) + D + J_0 - \frac{3}{2}H, \\ |F3\rangle &= \prod_{i=1}^N |v_{1,a}\rangle_i \otimes |\uparrow\rangle_i, \quad \varepsilon_{F3} = -\Delta(J - \Delta K) + D + J_0 - \frac{3}{2}H. \end{aligned} \quad (8)$$

There are also four another ferrimagnetic ground states with $M = 1/5$:

$$\begin{aligned} |F4\rangle &= \prod_{i=1}^N |v_{1,s}\rangle_i \otimes |\downarrow\rangle_i, \quad \varepsilon_{F4} = \Delta(J + \Delta K) + D - J_0 - \frac{1}{2}H, \\ |F5\rangle &= \prod_{i=1}^N |v_{1,a}\rangle_i \otimes |\downarrow\rangle_i, \quad \varepsilon_{F5} = -\Delta(J - \Delta K) + D - J_0 - \frac{1}{2}H, \\ |F6\rangle &= \prod_{i=1}^N |v_{0,a}\rangle_i \otimes |\uparrow\rangle_i, \quad \varepsilon_{F6} = -J + K + 2D - \frac{1}{2}H, \\ |F7\rangle &= \prod_{i=1}^N |v_{0,-}\rangle_i \otimes |\uparrow\rangle_i, \quad \varepsilon_{F7} = \frac{1}{2} \left(-J + (1 + 4\Delta^2)K + 2D - \sqrt{8\Delta^2(J - K)^2 + (J - K - 2D)^2} \right) - \frac{1}{2}H. \end{aligned} \quad (9)$$

When no external magnetic field is applied, there are also possibility of frustrated ground state formation, in which the orientation of σ spins in each block are not defined. In this case all σ spins become decoupled and behave like free spins. There are two frustrated ground states

$$\begin{aligned} |FR1\rangle &= \prod_{i=1}^N |v_{0,a}\rangle_i \otimes |\xi\rangle_i, \quad \varepsilon_{FR1} = -J + K + 2D, \\ |FR2\rangle &= \prod_{i=1}^N |v_{0,-}\rangle_i \otimes |\xi\rangle_i, \quad \varepsilon_{FR2} = \frac{1}{2} \left(-J + (1 + 4\Delta^2)K + 2D - \sqrt{8\Delta^2(J - K)^2 + (J - K - 2D)^2} \right). \end{aligned} \quad (10)$$

Here $|\xi\rangle_i$ stands for arbitrary value of the σ spin in the i -th block. Thus, for $H = 0$ if $S = 1$ dimer has $S_{tot}^z = 0$ then its neighboring σ -spins become decoupled which results in macroscopic non-zero entropy $S/N = \log 2$ for each of the frustrated ground states of Eq. 10. Applying magnetic field one removes the two-fold macroscopic degeneracy driving $|FR1\rangle$ and $|FR2\rangle$ ground states into $|F6\rangle$ and $|F7\rangle$ respectively. Nevertheless, in some papers two last non-degenerated ground states of eqs.(9) are mentioned as frustrated ones [14, 15, 16].

Hereafter, to discuss the phase diagrams we will consider the external magnetic field as $h_1=h_2=H$. In figure 2 the zero temperature ground state phase diagram are displayed in $(J/K, H/K)$ plane, for fixed values of, $J_0 = 1/2$, $D/K = 1$ and $\Delta = 3$. Eight possible states appear here, one ferromagnetic (fully polarized) state given by eq. (7), three ferrimagnetic states with magnetization $M = 3/5$, which are identified as F1, F2 and F3 states defined by eqs.(8), and

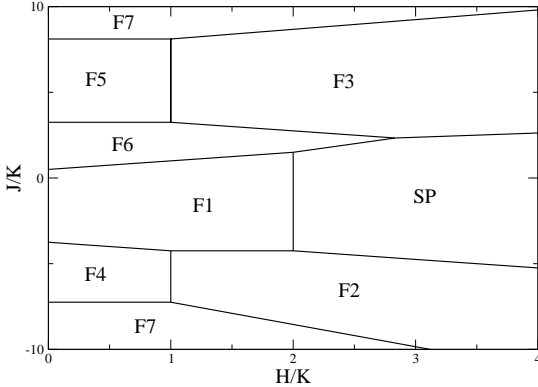


Figure 2: Phase diagram for J/K against H/K , for fixed values of, $J_0 = 1/2$, $D/K = 1$ and $\Delta = 3$.

finally this phase diagram also exhibit four ferrimagnetic states with magnetization $M = 1/5$, corresponding to F4, F5, F6 and F7 ground states given by eqs. (9). The phase transition boundary between F7 and F4 is a constant line $J/K = -29/4$, while the phase transition curve between F7 and F2 is expressed as $-\frac{14H/K+51+\sqrt{8433+3156H/K+292(H/K)^2}}{24}$, at this stage the diagram also exhibit a triple point for F2, F4 and F7 at $(H/K, J/K) = (1, -29/4)$. Then, we have found the phase transition line between F4 and F1 to be given by the equation $-\frac{1}{2}H/K - \frac{15}{4}$, the phase transition boundary between F1 and F2 is a constant horizontal line $J/K = -\frac{17}{4}$, and a triple point for F4, F2 and F1 is located at $(H/K, J/K) = (1, -17/4)$. The phase transition boundary between F2 and SP ground states is represented by the line $-\frac{1}{2}H/K - \frac{13}{4}$, on which another triple point appears for F1, F2 and SP at $(H/K, J/K) = (2, -17/4)$. The next phase boundary between ground states F1 and F6 is given by the line $(H/K + 1)/2$, the phase transition between states SP and F6 occurs when the $J/K = H/K - 1/2$, whereas the phase transitions line between SP and F3 ground states is given by $\frac{1}{4}H/K + \frac{13}{8}$. Yet another triple point occurs for SP, F3 and F6 at $(H/K, J/K) = (17/6, 7/3)$. The phase transition boundary between F3 and F6 ground states is limited by $-\frac{1}{2}H/K + \frac{15}{4}$, while the phase transition line between F6 and F5 ground states is a constant line at $J/K = \frac{13}{4}$, there is also additional triple point for F3, F5 and F6 at $(H/K, J/K) = (1, 13/4)$. In addition to that, we have found the phase transition line between F5 and F7 ground states to be another one constant line given by $J/K = 8.111$, and finally the phase transition curve between F3 and F7 is given by the expression $\frac{5(2H/K+33)+\sqrt{38889+6756H/K+292(H/K)^2}}{48}$, there is another triple point for ground states F3, F5 and F7 located at $(H/K, J/K) = (1, 8.111)$.

In figure 3 the phase diagrams for a fixed values of $D/J = 1$ and $\Delta = 1/2$ are plotted. The phase diagram corresponding to fixed values of biquadratic parameter $K/J = 1/2$ is displayed in figure 3(a) in $(J_0/J, H/J)$ parameters plane. Here one can distinguish the following eigenstates SP, F1, F2, F3, F5 and F7. First, let us consider the phase boundary between SP and F3 ground states which is given by the line $-23/8 + H/J$, whereas the phase transitions boundary between states SP and F1 is represented by the line $J_0/J = \frac{1}{4}H/J$, so the triple point for the states SP, F1 and F3 occurs at $(H/J, J_0/J) = (23/6, 23/24)$. Another phase transitions line exists between two ferrimagnetic ground states F1 and F3, $J_0/J = 23/24$, while the phase transition between the ground states F1 and F5 is given by $J_0/J = 23/8 - H/J$, one more triple point appear for F1, F3 and F5 at $(H/J, J_0/J) = (23/12, 23/24)$. The phase boundary between F3 and F5 is described by $J_0/J = \frac{1}{2}H/J$, whereas for the F3 and F7 ground state there is another straight line $J_0/J = -0.4542 + H/J$. Finally, the phase transition line between the ground states F5 and F7 is given by $J_0/J = -0.4542$, which terminates in yet another triple point, $(H/J, J_0/J) = (0.9083, 0.4542)$, for F3, F7 and F5.

The ground states phase diagram for fixed value of magnetic field $H/J = 1$ is displayed in figure 3(b) in the the parameters plane $(J_0/J, K/J)$. Here one can see the regions corresponding to the following ground states: SP, F1, F3, F5 and F7. The phase boundary between ground states states SP and F7 is given by the curve $J_0/J = -\frac{1+\sqrt{3-2K/J+3(K/J)^2}}{4}$, between SP and F3 - by the line $J_0/J = -\frac{3}{2}-\frac{3}{4}K/J$. There is a triple point for the ground states SP, F3 and F7 located at $(K/J, J_0/J) = (-0.8107, -0.892)$. The next phase transition curve, separating F3 and F7 is given by the equation $J_0/J = 1+\frac{3}{4}K/J-\frac{1}{2}\sqrt{3-2K/J+3(K/J)^2}$, while F3 and F5 is separated by a constant line at $J_0/J = 0.5$, here one can see also the triple point at $(K/J, J_0/J) = (0.4274, 0.5)$ in which F3, F5 and F7 coexist. The phase transition between F5 and F7 occurs in the curve given by $J_0/J = -\frac{3}{4}K/J+\frac{1}{2}\sqrt{3-2K/J+3(K/J)^2}$, the phase

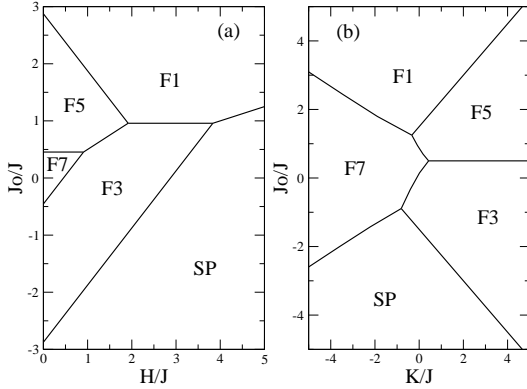


Figure 3: Ground states phase diagrams: (a) J_0/J vs. H/J , for a fixed values of $\Delta = 1/2$, $K/J = 1/2$ and $D/J = 1$; (b) J_0/J vs. K/J , for a fixed values of $\Delta = 1/2$, $H/J = 1$ and $D/J = 1$.

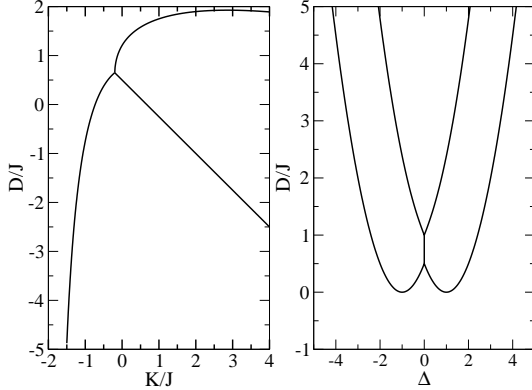


Figure 4: Phase diagrams: In (a) D/J versus K/J , for fixed values of $H/J = 1$, $J_0/J = 1$ and $\Delta = 1/2$. In (b) D/J versus Δ , for fixed values of $H/J = 1$, $J_0/J = 1$ and $K/J = 1/2$.

boundary between ground states $F1$ and $F5$ is described by $J_0/J = \frac{3}{2} + \frac{3}{4}K/J$, and finally the phase boundary among states $F1$ and $F7$ is represented by $J_0/J = \frac{3+\sqrt{3-2K/J+3(K/J)^2}}{4}$. The triple point occurs at $(K/J, J_0/J) = (-1/3, 5/4)$, where $F1$, $F5$ and $F7$ merge.

The figure 4 is devoted to the phase diagram for a fixed values of $H/J = 1$ and $J_0/J = 1$. One can see the phase diagram in the plane D/J versus K/J in figure 4(a) where fixed value of $\Delta = 1/2$ is assumed. There are three phases that appear in that case. The phase boundary between $F1$ and $F5$ is given by the line $D/J = \frac{1}{2} - \frac{3}{4}K/J$, while the boundary between ground states $F1$ and $F7$ is expressed as $D/J = -\frac{3(K/J)^2-2K/J-2}{2+K/J}$, and boundary transition between $F5$ and $F7$ is given by the curve $D/J = \frac{1-K/J}{2} + \frac{1}{4}\sqrt{(K/J)^2 + 40K/J + 8}$. There is only one triple point in the diagram located at $(K/J, D/J) = (0.2, 0.65)$.

Further, the phase diagram of the system under consideration for a fixed value of $K/J = 1/2$ is displayed in $(D/J, \Delta)$ -plane in figure 4(b). In this case the following ground states appear: $F1$, $F4$, $F5$ and $F7$. The phase transition line between $F1$ and $F5$ is given by the curve $D/J = (1 - \Delta)^2/2$, while those for $F1$ and $F4$ is given similarly by $D/J = (1 + \Delta)^2/2$, the other phase boundary between $F4$ and $F7$ can be expressed as $D/J = \frac{1+\sqrt{9-24\Delta+20\Delta^2-16\Delta^3+4\Delta^4}}{4}$, while ground states $F5$ and $F7$ are separated by the curve $D/J = \frac{1+\sqrt{9+24\Delta+20\Delta^2+16\Delta^3+4\Delta^4}}{4}$. In this case, phase diagram contain two triple points, for $F1$, $F5$ and $F4$ located at $(\Delta = 0, D/J = 0.5)$ and for $F4$, $F5$ and $F7$ at $(\Delta = 0, D/J = 1)$.

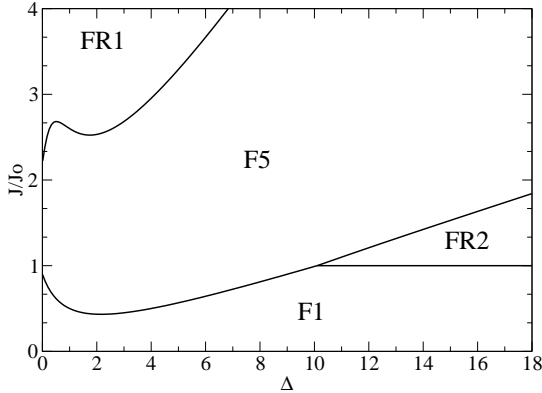


Figure 5: Phase diagram in $(\Delta, J/J_0)$ -plane for fixed $D/J_0 = 0$, small values of $K/J_0 = 0.1$ and null zero magnetic field $H/J_0 = 0$.

In order to demonstrate appearance of the frustrated state given by eq.(10) the zero temperature and zero field phase for parameters Δ versus J/J_0 is presented in figure 5, here we also put with $D = 0$ and consider a small contribution of biquadratic coupling $K/J_0 = 0.1$. Obviously, any non-zero magnetic field destroys frustrated ground states FR1 and FR2 driving them by aligning σ -spins into F6 and F7 ground states respectively. Note, that σ -spins are decoupled in the frustrated states. Beside frustrated ground states the phase diagram contains also F1 and F5 which are separated by line given by $J/J_0 = \frac{1-\tilde{K}+\tilde{K}\Delta^2}{1+\Delta}$ (with $\tilde{K} = K/J_0$). The boundary between F1 and frustrated state FR2 is a constant line $\tilde{K} = 1$, while the boundary between frustrated state FR2 and state F5 is represented by $J/J_0 = \frac{-\tilde{K}-1+\tilde{K}\Delta^2}{-1+\Delta}$ and finally the boundary between state F5 and frustrated state FR1 is given by the following function $J/J_0 = \tilde{J} = \tilde{K}(1+2\Delta) + \frac{2\Delta-1}{\Delta(1+\Delta)} + \frac{(1+\tilde{K}\Delta+\tilde{K}\Delta^2)\sqrt{1+8\Delta^2}}{\Delta(1+\Delta)}$. The triple point for F1, FR2 and F5 is located at $(\Delta = 10.09901951, \tilde{J} = 1.0)$.

4 Exact Solution and Thermodynamics

The present model could be solved exactly using the known decoration transformation early presented by M. E. Fisher[18, 19], and recently generalized for arbitrary spin interactions[20], where one maps the partition function of the system to the partition function of 1d Ising model, writing down the relations for the entries of transfer matrix and thus obtaining the relations between model parameters and that of Ising chain. But here we implement a direct transfer matrix calculations without any account to the solution of Ising chain. Therefore let us consider the following partition function of the system, which can be represented as

$$\mathcal{Z} = \sum_{\sigma} \text{Sp}_{\sigma} \exp(-\beta \mathcal{H}) = \sum_{\sigma} \prod_{i=1}^N \exp(\beta \frac{h_2}{2}(\sigma_i + \sigma_{i+1})) Z(\sigma_i, \sigma_{i+1}), \quad (11)$$

where β as usual is inverse temperature.

At this stage one can easily observe that the structure of relation implies the possibility of introducing the decoration–iteration transformation[18, 20] known as the *partial* partition function or Boltzmann weight, for one quantum dimer reads

$$Z(\sigma_i, \sigma_{i+1}) = \text{Sp}_i \exp(-\beta \mathcal{H}_i) = \sum_{n=1}^9 \exp(-\beta \lambda_n(\sigma_i, \sigma_{i+1})). \quad (12)$$

Then, the *partial* partition function (12) corresponding to one block can be easily expressed in the following form

$$\begin{aligned}
Z(\sigma_i, \sigma_{i+1}) &= \sum_{n=0}^2 Z_n \cosh(\beta n(h_1 - J_0(\sigma_i + \sigma_{i+1}))), \\
Z_0 &= e^{\beta(J-K-2D)} + 2e^{\beta\frac{1}{2}(J-(1+4\Delta^2)K-2D)} \cosh\left(\beta\frac{1}{2}\sqrt{8\Delta^2(J-K)^2 + (J-K-2D)^2}\right), \\
Z_1 &= 4e^{-\beta(\Delta K+D)} \cosh(\beta\Delta J), \\
Z_2 &= 2e^{-\beta(J+K+2D)}.
\end{aligned} \tag{13}$$

After that, one can represent the partition function (11) in the similar form to the partition function of a chain with classical two state variables on each site:

$$\mathcal{Z} = \sum_{\sigma} \prod_{i=1}^N T(\sigma_i, \sigma_{i+1}) = \text{Sp} \mathbf{T}^N = \Lambda_1^N + \Lambda_2^N, \tag{14}$$

where $\Lambda_{1,2}$ are two eigenvalues of the transfer-matrix \mathbf{T} which takes the following form

$$\mathbf{T} = \begin{pmatrix} e^{\beta\frac{h_2}{2}} \mathcal{Z}_+ & \mathcal{Z}_0 \\ \mathcal{Z}_0 & e^{-\beta\frac{h_2}{2}} \mathcal{Z}_- \end{pmatrix}, \tag{15}$$

where

$$\begin{aligned}
\mathcal{Z}_{\pm} &= Z(\pm 1/2, \pm 1/2), \\
\mathcal{Z}_0 &= Z(1/2, -1/2) = Z(-1/2, 1/2).
\end{aligned} \tag{16}$$

Then, calculating the eigenvalues and taking thermodynamic limit, when only the largest eigenvalue survives, one arrives at the following expression for the free energy per block:

$$f = -\frac{1}{\beta} \log \left(\frac{1}{2} \left(e^{\beta\frac{h_2}{2}} \mathcal{Z}_+ + e^{-\beta\frac{h_2}{2}} \mathcal{Z}_- + \sqrt{(e^{\beta\frac{h_2}{2}} \mathcal{Z}_+ - e^{-\beta\frac{h_2}{2}} \mathcal{Z}_-)^2 + 4\mathcal{Z}_0^2} \right) \right). \tag{17}$$

As soon as the free energy per block is calculated, one can obtain analytic expressions for all thermodynamic function.

4.1 Magnetization and quadrupole moment

Magnetic quantities can be obtained using the free energy expression obtained in (17). Therefore the magnetization of the spin- S can be expressed as

$$M_S = \frac{1}{2N\mathcal{Z}} \sum_{\sigma} \text{Sp}_S \left(\sum_{i=1}^N (S_{i1}^z + S_{i2}^z) e^{-\beta\mathcal{H}} \right) = -\frac{1}{2} \left(\frac{\partial f}{\partial h_1} \right)_{\beta, h_2, D}, \tag{18}$$

while the magnetization of spin- σ read as

$$M_{\sigma} = \frac{1}{N/2\mathcal{Z}} \sum_{\sigma} \text{Sp}_S \left(\sum_{i=1}^N \sigma_i e^{-\beta\mathcal{H}} \right) = -2 \left(\frac{\partial f}{\partial h_2} \right)_{\beta, h_1, D}. \tag{19}$$

Thus the total magnetization is given by

$$M = \frac{1}{5} M_{\sigma} + \frac{4}{5} M_S. \tag{20}$$

Figure 6(a) displays the plot of magnetization as a function of biquadratic interaction term K for fixed values of $H = 2.5$, $J_0 = 1/2$, $T = 0.1$, $\Delta = 3$ and $D = 1$. Here one can see the plateaus for different values of J , this plateaus occur as expected at $1/5$ and $3/5$. The plots of magnetization processes (M versus H) for the system under consideration is presented in figure 6(b). Here the values of parameters are fixed as $K = -1/6$, $J_0 = 1/2$, $T = 0.15$, $\Delta = 3$ and $D = 1$ and value of J varies from -2 to 2 . When $J = \pm 2$ (solid and dotted lines) the magnetization curves display two intermediate plateaus at $M = 1/5$ and $M = 3/5$, while for $J = \pm 1$ one see only one plateau at $M = 1/5$ (dashed and dot-dashed lines). Thermal behavior of magnetization at the fixed external field is presented in figure 6(c)

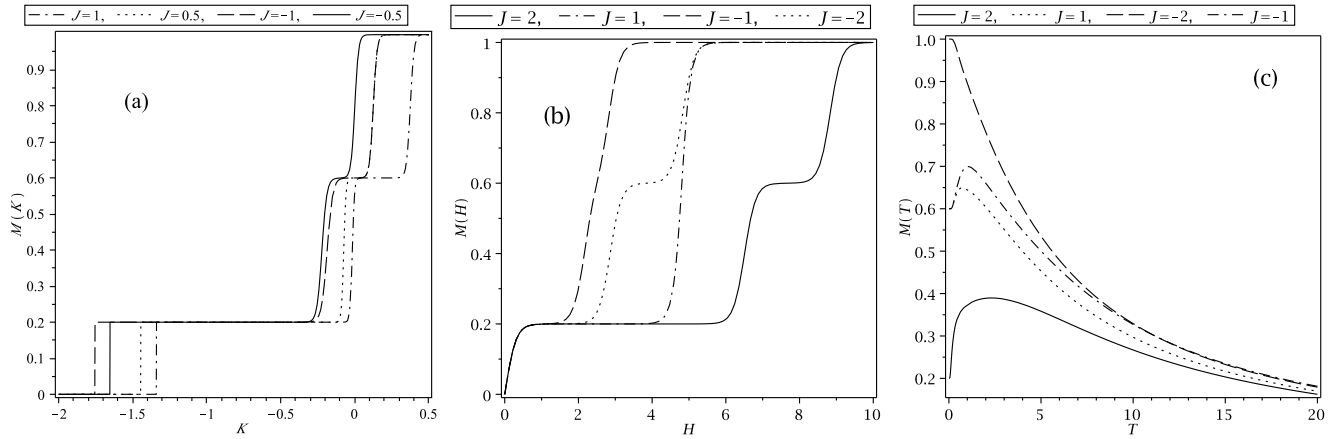


Figure 6: (a) Magnetization as a function of K , for $H = 2.5$, $J_0 = 1/2$, $T = 0.1$, $\Delta = 3$ and $D = 1$. (b) Magnetization as a function of H , for $K = -1/6$, $J_0 = 1/2$, $T = 0.15$, $\Delta = 3$ and $D = -1$. (c) Magnetization versus temperature T , for $K = -1/6$, $H = 6$, $J_0 = 1/2$, $\Delta = 3$ and $D = 1$.

where the following values of parameters are assumed: $K = -1/6$, $J_0 = 1/2$, $H = 6$, $\Delta = -1$ and $D = 1$, where display the competition effect between ferromagnetic state SP and ferrimagnetic state F1 with magnetization $M = 3/5$, when temperature increases. Close to zero temperature one obtains three well defined values for the magnetization, which are in accordance with plateaus displayed in figure 6(a-b).

As the system under consideration contains sites with $S = 1$ one can define another important physical quantity, quadrupole moment, which can be obtained by the thermodynamic relations as well

$$Q = \frac{1}{2N\mathcal{Z}} \sum_{\sigma} \text{Sp}_{\mathbf{S}} \left(\sum_{i=1}^N ((S_{i1}^z)^2 + (S_{i2}^z)^2) e^{-\beta \mathcal{H}} \right) = \frac{1}{2} \left(\frac{\partial f}{\partial D} \right)_{\beta, h_1, h_2}. \quad (21)$$

Some properties of the quadrupole moment also will be discussed due to the contribution of the biquadratic and uniaxial single-ion anisotropy parameters.

In figure 7(a) the plots of quadrupole moment as a function of K for fixed values of $H = 0$, $J = 1$, $J_0 = 1$, $\Delta = 3$ and $D = -1$ are presented for several temperatures. The non-trivial and non-monotone behavior of Q under variation of K can be understood if one take into account appearance of F7 and FR2 ground states in which vertical quantum dimer is in $|v_{0,-}\rangle$ eigenstate. Calculating expectation value for the operator Q for this state one obtains:

$$\langle v_{0,-} | \frac{1}{2} ((S_1^z)^2 + (S_2^z)^2) | v_{0,-} \rangle = \frac{2}{2 + \frac{1}{4\Delta^2} \left(1 + \frac{2D - \sqrt{8\Delta^2(J-K)^2 + (J-K-2D)^2}}{K-J} \right)^2}, \quad (22)$$

which actually defines low-temperature behavior of the quadrupole moment. The quadrupole moment dependence of the uniaxial single-ion anisotropy parameter D is illustrated in figure 7(b), assuming $H = 2.5$, $J = 0.5$, $T = 0.1$, $\Delta = 3$ and $D = 1$. Similar to the case of the magnetization we obtain some plateaus, but for higher values of D we have a decreasing curve instead of plateaus (solid line). On the other hand, as soon as the temperature increases these plateaus obviously disappear. Whereas in figure 7(c) we plot the quadrupole moment as a function of the temperature for fixed values of $J = -1$, $K = 0.5$, $H = 0$, $J_0 = 0.5$ and $\Delta = 3$, similar to the case of magnetization (fig.6(c)), the quadrupole moment leads to fixed values at low temperature which are related to the plateaus displayed in figures 7(a-b), while at high temperature average quadrupole moment leads to $2/3$, which corresponds to equal probabilities for all three values of $S = 1$ spin.

4.2 Entropy and specific heat

The entropy of the system can be obtained according to general thermodynamic relation,

$$S(T) = - \left(\frac{\partial f}{\partial T} \right)_{h_1, h_2, D}. \quad (23)$$

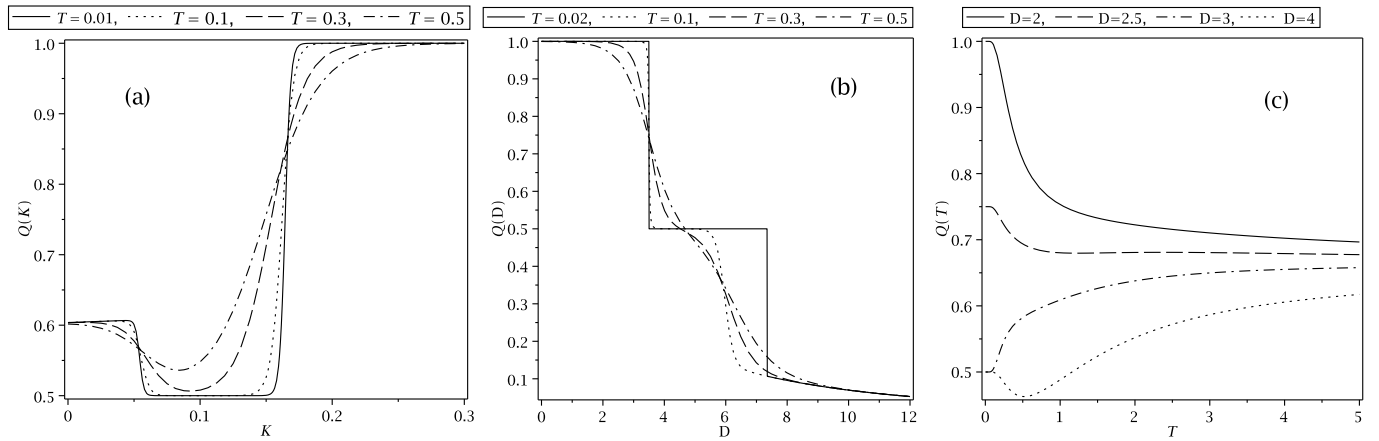


Figure 7: Quadrupole Moment: (a) As a function of K , for $H = 0$, $J = 1$, $J_0 = 1$, $\Delta = 3$ and $D = -1$. (b) As a function of D , for $J = -1$, $K = 0.5$, $H = 1.5$, $J_0 = 0.5$ and $\Delta = 3$. (b) As a function of T , for $J = -1$, $K = 0.5$, $H = 0$, $J_0 = 0.5$ and $\Delta = 3$.

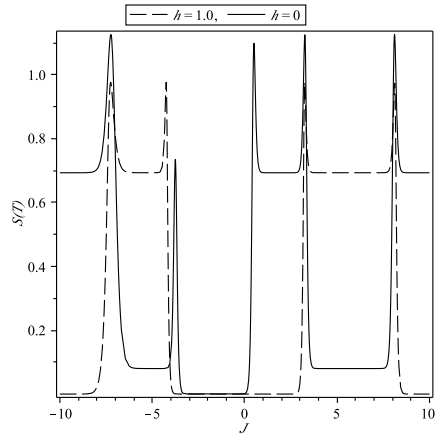


Figure 8: The entropy $S(T)$ against J : assuming fixed values for $K = 1$, $J_0 = 0.5$, $T = 0.1$, $\Delta = 3$, $D = 1$ and $H = 1$ (dashed line), and $H = 0$ (solid line).

One can see the plot of entropy $S(T)$ of the model as a function of J in figure 8, here we fix the following values of the parameters: $K = 1$, $J_0 = 0.5$, $T = 0.1$, $\Delta = 3$ and $D = 1$, assuming the external magnetic field is $H = 1$ (dashed line) and external magnetic field is zero (solid line). A series of peaks corresponding to quantum phase transition points appear on the curve which is in accordance with the phase transition at zero temperature illustrated in figure 2. According to previous discussion, when external magnetic field vanishes there are a residual entropy of the model corresponding to frustrated ground states. This residual entropy is a constant value $S(0) = \ln(2) = 0.693$ related to the ground state degeneracy. For particular values of the magnetic field like $H = 1$ also it is possible to see that the ground state energy is twofold degenerate, as we can verify in figure 2, residual entropy for some intervals of J appears as we can verify in figure 8.

Using the entropy $S(T)$, one can obtain the specific heat

$$C = T \left(\frac{\partial S}{\partial T} \right). \quad (24)$$

In order to study the specific heat properties for the model under consideration, we display the specific heat as a function of the parameter K for the fixed values of $J = -1$, $H = 1$, $T = 0.2$, $J_0 = -0.5$, $\Delta = 3$ and $D = 1$. In figure 9 the corresponding plot exhibits four peaks which are related to the phase transition at zero temperature. As one can see the phase transition effects appears for small values of the biquadratic term K .

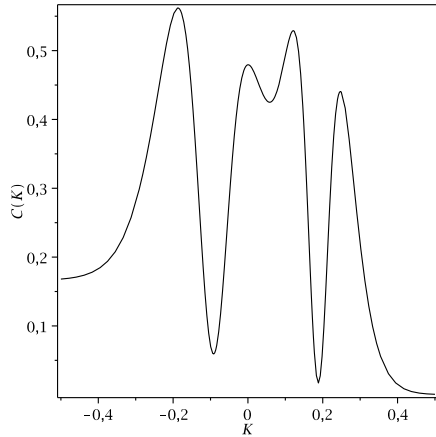


Figure 9: The specific heat $C(T)$, for the fixed values of $J = -1$, $H = 1$, $T = 0.2$, $J_0 = -0.5$, $\Delta = 3$ and $D = 1$.

5 Conclusions

We have considered an exactly solvable variant of diamond chain with mixed $S = 1$ and $S = 1/2$ spins. The vertical $S = 1$ dimers are taken as quantum ones with Heisenberg bilinear and biquadratic interactions and with single-ion anisotropy terms, while all interactions between $S = 1$ spins and $S = 1/2$ spins residing on the intermediate sites are taken in the Ising form. The model generalizes the model of diamond chain with Ising and Heisenberg bonds considered in [29]. Our results supplement the previously obtained ones for the case of $S = 1$ vertical XXZ-dimers with only bilinear Heisenberg interaction. The detailed analysis of the $T = 0$ ground state phase diagrams is presented as well as the exact plots of various thermodynamic functions. The effect of biquadratic term and single-ion anisotropy are summarized in the corresponding phase diagrams. The phase diagrams have shown to be rather rich, demonstrating large variety of ground states: saturated one, three ferrimagnetic with magnetization equal to $3/5$ and another four ferrimagnetic ground states with magnetization equal to $1/5$. There are also two frustrated macroscopically degenerated ground states which could exist at zero magnetic field. The thermodynamic properties of the model have been described exactly by exact calculation of partition function within the direct classical transfer-matrix formalism, the entries of transfer matrix, in their turn, contain the information about quantum states of vertical $S = 1$ XXZ dimer (eigenvalues of local hamiltonian for vertical link). The plots of entropy and specific heat are also presented.

Acknowledgments

V.O. express his gratitude to Institut für Theoretische Physik Universität Göttingen for warm hospitality during the final stage of this work. This research stay was supported by DFG (Project No. HO 2325/7-1). V.O and M. K. were partly supported by the joint grant of CRDF and State Committee of Science of Republic of Armenia ECSP-09-94-SASP, the work of V. O. was also partly supported by Volkswagen Foundation (grant No. I/84 496) and ANSEF-1981-PS. O.R. and S.M.S thanks CNPq and FAPEMIG for partial financial support.

References

- [1] F. Aimo, S. Krüger, M. Klajic, M. Horvatic, C. Berthier, H. Kikuchi, Phys. Rev. Lett. **102**, 127205 (2009).
- [2] K. C. Rule, A. U. B. Wolter, S. Sütő, D. A. Tennant, A. Brügel, S. Kühneler, B. Wolf, M. Lang, J. Schreuer, Phys. Rev. Lett. **100**, 117202 (2008).
- [3] H. Kikuchi, Y. Fujii, M. Chiba, S. Mitsudo, T. Idehara, T. Tonegawa, K. Okamoto, T. Sakai, T. Kuwai, H. Ohta, Phys. Rev. Lett. **94**, 227201 (2005).
- [4] B. Gu and G. Su, Phys. Rev. B **97**, 174437 (2007).
- [5] K. Hida, K. Takano, and H. Suzuki, J. Phys. Soc. Jpn. **78**, 084716 (2009).

- [6] K. Takano, H. Suzuki, and K. Hida, Phys. Rev. B **80**, 104410 (2010).
- [7] T. Sakai, K. Okamoto, and T. Tonegawa, J. Phys. : Conf. Series **200**, 022052 (2010).
- [8] N. B. Ivanov, J. Richter, and J. Schulenburg, Phys. Rev. B **79**, 104412 (2009).
- [9] H. H. Fu, K. L. Yao, Z. L. Liu, Phys. Rev. B **73**, 104454 (2006).
- [10] M. S. S. Pereira, F. A. B. F. de Moura, M. L. Lyra, Phys. Rev. B **77** 024402 (2008).
- [11] M. S. S. Pereira, F. A. B. F. de Moura, M. L. Lyra, Phys. Rev. B **79** 054427 (2009).
- [12] O. Derzhko, A. Honecker, and J. Richter, Phys. Rev. B **79**, 054403 (2009).
- [13] J. S. Valverde, O. Rojas, and S. M. de Souza, Physica A **387**, 1947 (2008).
- [14] L. Čanovíč, J. Strečka, and M. Jačočur, J. Phys. : Condens. Matter **18**, 4967 (2006).
- [15] L. Čanovíč, J. Strečka, T. Lučivjanský, Condensed Matter Physics **12**, 353 (2009).
- [16] J. Strečka, L. Čanovíč, T. Lučivjanský, and M. Jačočur, J. Phys. : Conf. Series **145**, 012058 (2009).
- [17] T. Verkholyak, J. Strečka, M. Jačočur, and J. Richter *Magnetic properties of the quantum spin-1/2 XX diamond chain: The Jordan–Wigner approach*, arXive: 1004.0848 (2010).
- [18] M.E. Fisher; Phys. Rev. **113**, 969 (1958).
- [19] Syozi, I. *Phase Transitions and Critical Phenomena*, 1, pp. 269-329. Edited by Domb C. and Green M.S., Academic Press, New York, (1972).
- [20] O. Rojas, J.S. Valverde and S.M. de Souza, Physica A **388**, 1419 (2009).
- [21] H. Kobayashi, Y. Fukumoto, and A. Oguchi, J. Phys. Soc. Jpn. **78**, 074004 (2009).
- [22] T. A. Arakelyan, V. R. Ohanyan, L. N. Ananikyan, N. S. Ananikian, M. Roger, Phys. Rev. B **67**, 024424 (2003).
- [23] J. S. Valverde, O. Rojas, and S. M. de Souza, J. Phys.: Condens. Matter **20**, 345208 (2008).
- [24] V. Hovhannisyan and N. Ananikian, Phys. Lett. A **372**, 3363 (2008).
- [25] D. Antonosyan, S. Bellucci, V. Ohanyan, Phys. Rev. B **79**, 014432 (2009).
- [26] V. Ohanyan, Phys. Atom. Nucl. **73**, 494 (2010).
- [27] V. Ohanyan, Condensed Matter Physics **12**, 343, (2009).
- [28] S. Bellucci and V. Ohanyan, Eur. Phys. J. B **75**, 531 (2010).
- [29] J. Strečka, M. Jačočur, M. Hagiwara, Y. Narumi, K. Kindo and K. Minami, Phys. Rev. B **72**, 024459 (2005).
- [30] V. Ohanyan and N. Ananikian, Phys. Lett. A **307**, 76 (2003).
- [31] F. Litaiff, J. Desousa, and N. Branco, Solis State Commun. **147**, 494 (2008).
- [32] D. Visinescu, A. M. Madalan, M. Andruh, C. Duhayon, J.-P. Sutter, L. Ungur, W. Van der Heuvel, and L. F. Chibotaru, Chem. Eur. J. **15**, 11808 (2009).
- [33] C. Kittel, Phys. Rev. **120**, 335 (1960).
- [34] R. Baxter, *Exactly Solved Models in Statistical Mechanics*, (Academic Press, New York, 1982).